Pulsed metal-organic chemical vapor deposition of high-quality AlN/GaN superlattices for near-infrared intersubband transitions

C. Bayram, N. Péré-laperne, R. McClintock, B. Fain, and M. Razeghi[a)]
Department of Electrical Engineering and Computer Science, Center for Quantum Devices, Northwestern University, Evanston, Illinois 60208, USA

(Received 13 January 2009; accepted 4 March 2009; published online 23 March 2009)

A pulsed metal-organic chemical vapor deposition technique is developed for the growth of high-quality AlN/GaN superlattices (SLs) with intersubband (ISB) transitions at optical communications wavelengths. Tunability of the AlN and GaN layers is demonstrated. Indium is shown to improve SL surface and structural quality. Capping thickness is shown to be crucial for ISB transition characteristics. Effects of barrier- and well-doping on the ISB absorption are reported. © *2009 American Institute of Physics*. [DOI: 10.1063/1.3104857]

Intersubband (ISB) transitions are excellent mechanism for ultrafast optical switches since the ISB relaxation time can be three orders of magnitude smaller than that of interband.[1] Wide-bandgap AlN/GaN superlattice (SL) has a large conduction-band offset[2] ($\sim$2.1 eV) suitable for near-infrared ISB devices, and has the potential to offer tunability over the complete optical communications wavelength region (1.3–1.6 μm) for applications including multiterabit optical time division multiplexed networks as well as chemical/biological sensing.

Due to large electron effective mass [$m^* \sim (0.2-0.3) \times m_0$] and the large longitudinal optic (LO) phonon energy ($\sim$90 meV), ISB transition speeds in (Al)GaN wells are on the order of a few hundred femtoseconds[3] whereas that of InGaAs are around 2–5 ps at 1.55 μm.[4] Thus from a device physics standpoint, among the proposed materials (such as AlAs/InGaAs, AlAsSb/InGaAs, and BeTe/ZnSe SLs), AlN/GaN SLs are the most promising choice for high-performance near-infrared ISB devices.[2,4] However, due to the lack of readily available lattice matched substrates, the growth of AlN/GaN SL proves challenging.

Molecular beam epitaxy has been used to realize AlN/GaN SL absorbing at optical communications wavelengths.[5] However, there are few reports for metal-organic chemical vapor-phase epitaxy (MOCVD)-grown AlN/GaN SL absorbing in near-infrared[6] and fewer leading to absorption around 1.55 μm.[7,8] Today, most nitride based commercial optoelectronic devices are grown by MOCVD. Thus, there is a wide interest to realize high-quality ISB absorption at telecommunication wavelengths by MOCVD.

The AlN/GaN SL, despite the lattice mismatch of 2.4%, can be realized crack-free and be grown pseudomorphically.[9] However III-nitrides are piezoelectric materials, in conventional *c*-plane growth. These highly strained layers generate multi-MV/cm electric fields.[10] Thus, interfaces or SL thickness fluctuations degrade the absorption quality significantly.[10] Another problem is AlN/GaN or GaN/AlN interface stability, and their dependence on (GaN or AlN) template.[11,12] Moreover, the embedded GaN layer gets thinner during subsequent AlN growth.[13] MBE-grown SLs have achieved shorter ISB transition wavelengths (as short as 1.08 μm)[14] than MOCVD-grown ones.[8] All these observations necessitate further MOCVD growth studies. In this work, we propose and analyze pulsed MOCVD deposition of AlN/GaN SL, and demonstrate ISB absorption at telecommunication wavelengths—the shortest wavelengths reported via MOCVD growth. The effect of well and barrier doping, and capping layer thickness on ISB absorption characteristics are also reported.

The material was grown in an AIXTRON 200/4-HT horizontal flow low-pressure MOCVD reactor. The template, consisted of a high-quality AlN layer, was grown on double-side polished (001) sapphire.[15] Trimethlyaluminum (TMAl), trimethylgallium (TMGa), and trimethlyindium (TMIn) are used as the metal-organic precursors for Al, Ga, and In, respectively. Ammonia (NH_3) and hydrogen are used as the anion source and carrier gas, respectively. Silane (SiH_4) is used as the *n*-type dopant source. All SL growth is performed at a pressure of 50 mbar and a temperature of 1035 °C.

Using conventional MOCVD growth, parasitic prereactions[16] between the TMAl and NH_3 necessitate lower pressures and smaller V/III ratios. The lack of aluminum adatom mobility also urges higher growth temperatures for AlN growth. In contrast, GaN typically obtains higher quality when grown under higher pressures and larger V/III ratios with moderate temperatures. The challenge in realizing high-quality SLs for ISB transitions is to find growth conditions that work simultaneously for both of these materials and yield well defined interfaces. One way to deposit GaN with a high V/III ratio, while decreasing the parasitic prereactions when depositing AlN, is to use temporal separation of TMAl and NH_3. This enhances the surface adatom migration and maximizes the growth efficiency.[17]

The proposed SL deposition technique has four steps, as shown in Fig. 1. Steps (I) and (II) result in AlN deposition. The separate introduction of the group III and V precursors into the growth chamber in an alternating sequence enhances the diffusion length of aluminum adatoms leading to higher quality material. Step (III) deposits GaN using conventional bulk deposition to ensure a high V/III ratio. Step (IV) nitridizes the surface before aluminum deposition for the next SL period. This step prepares the surface for AlN regrowth by eliminating the excess gallium on the interface that may otherwise form an AlGaN interlayer, thus degrading the interface sharpness. By this four-step SL deposition technique, V/III ratio for AlN is decreased whereas that of GaN is maxi-

[a)]Electronic mail: razeghi@eecs.northwestern.edu.

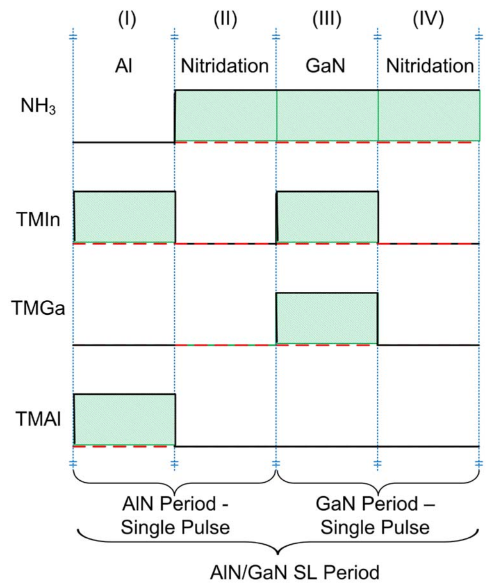

FIG. 1. (Color online) The growth sequence of AlN/GaN SL. One period consists of two main deposition phases: (1) AlN deposition, which is realized via pulsing TMAl and NH_3 to enhance aluminum adatom mobility [steps (I) and (II)], and (2) conventional GaN deposition [step (III)], which is realized by conventionally supplying TMGa and NH_3 simultaneously. Step IV nitridizes the surface.

mized and higher AlN growth rate and aluminum adatom mobility is achieved. A typical sketch of the SL is given in the inset of Fig. 2(a).

In order to further enhance the adatom mobility and realize high-quality SLs, the use of indium (as a nonincorporating surfactant) is investigated.[18] TMIn, is supplied along with TMAl and TMGa, as shown in Fig. 1, to increase the mobility of the aluminum and gallium adatoms. The insets of Figs. 2(b) and 2(c) show the atomic force microscopy (AFM) images of the surface of a SL grown without and with TMIn flow, respectively. The (1×1 μm^2) root-mean-square roughness decreased from 1.6 to 1.2 Å with the use of indium. The dark spots in the AFM, corresponding to surface termination of screw-type dislocations, also decreased. In order to assess the structural properties, open detector omega/2theta (002) x-ray diffraction (XRD) scans are performed. When TMIn is introduced, as in Fig. 1, the full width at half-maximum of the first and second order SL satellite peaks decrease significantly. All these results demonstrate that indium acts as a surfactant (indium incorporation is ~2%) and improves the overall SL quality in this technique.

Tunability of the well (GaN) and barrier (AlN) thickness are studied by growing AlN/GaN SL [as in the Fig. 2(a) inset] via varying the number of AlN pulses, GaN pulses or the amount of GaN deposition time (for a single GaN pulse) (as in Fig. 1). One AlN (GaN) pulse is steps I (III) and II (IV) for a given TMAl (TMGa) deposition time [step I (III)]. XRD is used to characterize the SL. The angular separation between satellite peaks are used to calculate the SL period.[19] The average aluminum composition was calculated via $x_{\mathrm{Al}} = (C_{\mathrm{AlGaN}} - C^0_{\mathrm{GaN}})/(C^0_{\mathrm{AlN}} - C^0_{\mathrm{GaN}})$ where C^0_{GaN} and C^0_{AlN} are the freestanding lattice parameters of GaN and AlN, and C_{AlGaN} is the average lattice constant of the SL determined from x-ray analysis.[19] 50 periods of various SL samples are grown, and layer thicknesses are deducted. Figure 2(a) displays the AlN thickness dependency on the number of AlN pulses. Similarly, GaN thickness dependency on GaN pulses and GaN deposition time are plotted in Figs. 2(b) and 2(c), respectively. AlN (or GaN) thickness was found to be a linear function of AlN (or GaN) pulses. However, the linear fits to GaN thickness [Figs. 2(b) and 2(c)] intersect ordinate below abscissa, which is attributed to the thinning of the GaN wells at high temperatures during subsequent AlN deposition.[13] Consequently, for the linear fit to AlN thickness [Fig. 2(a)], the intersection with ordinate is above abscissa. However, a linear deposition growth rate with respect to AlN (or GaN) pulses and GaN deposition time is determined that makes this technique feasible for controllable AlN/GaN SL.

The capping of the SL (50 periods of {1.9-nm-thick GaN/3.2-nm-thick AlN}) has been studied via photoluminescence (PL). Room temperature PL measurements are realized via frequency doubled argon-ion laser at 244 nm. Figure 3 shows the PL spectra of uncapped, 30, and 100 nm (AlN) capped SLs whereas inset shows the XRD (002) omega/2theta scans. Uncapped SLs are crack-free whereas few edge cracks are observed for the 30 nm capping, and become more prominent for the 100 nm capping (not shown). Thus, the significant blueshift observed with increasing capping is attributed to partial strain relief via crack formation. Consequently, XRD satellite peaks are better defined for (crack-free) uncapped sample with respect to (cracked) capped ones. With the crack formation, no significant period change is observed, however, the zeroth order peak of SL moved toward the AlN template peak—an indicator of strain relief occurring. The PL intensity increases for capped SLs, which

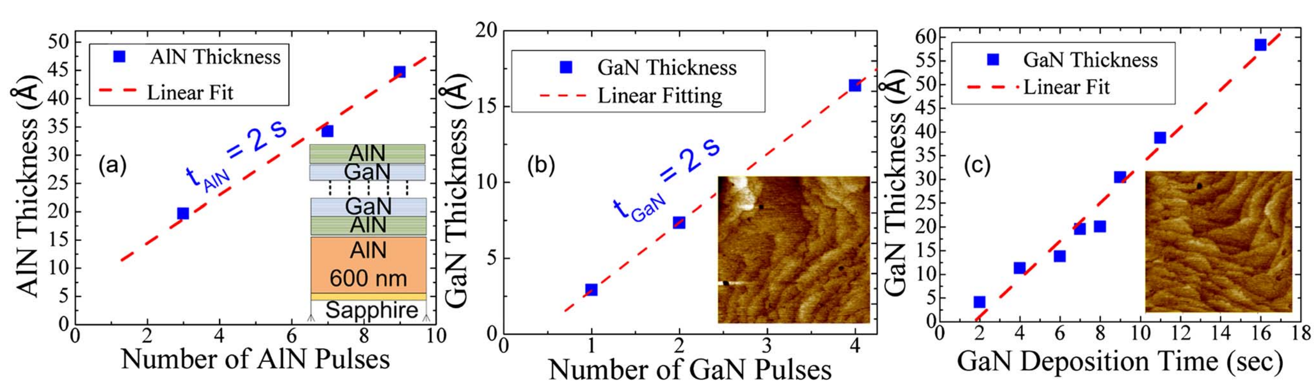

FIG. 2. (Color online) (a) AlN thickness vs number of AlN pulses for TMAl duration of 2 s. Inset shows a cross-sectional diagram of a SL. (b) GaN thickness vs number of GaN pulses for TMGa duration of 2 s. Inset shows the (1×1 μm^2) AFM SL surface without TMIn (height scale=1.5 nm). (c) GaN thickness vs TMGa duration for a single GaN pulse. Inset shows the (1×1 μm^2) AFM SL surface with TMIn (height scale=1.5 nm).

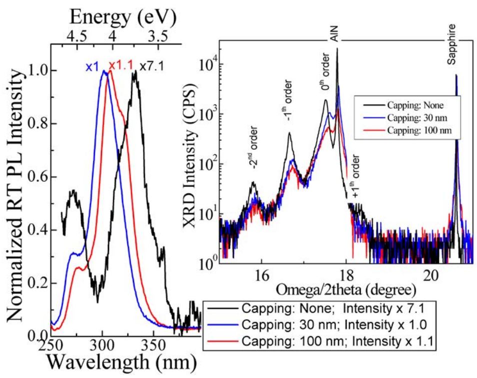

FIG. 3. (Color online) Room temperature PL of 50 periods {1.9-nm-thick GaN/3.2-nm-thick AlN} SL with different AlN capping thicknesses (uncapped, 30, and 100 nm). Inset shows (002) omega/2theta XRD of the SL with the different capping thicknesses.

we attribute to the partial doping effect via band bending due to the AlN capping layer.[20]

The N-type doping is realized by introducing SiH_4 along with metal-organic cation sources. SLs with the same amount of dopants either in the barrier or well are grown and no significant structural differences are observed by XRD or AFM.

Samples were prepared for ISB absorption measurements by dicing to allow transverse optical access to the layers. p- or s-polarized white light was incident perpendicular to one side facet of the samples, traveled along the SL region and went out from the other facet.[5] The infrared transmission was measured at room temperature using a Fourier transform infrared spectrometer. The difference between the absorption of p- and s-polarized light was used to identify ISB absorption. Figure 4 displays the transmission of the p-polarized light for uncapped, 30, and 100 nm capped SLs, as well as undoped, well-, or barrier-doped (n-type) samples. For uncapped samples, a weak absorption is observed. With 30 nm capping, the absorption is significantly increased. This is attributed to the unintentional doping generated by band bending with AlN capping,[20] and supports the increase in PL intensity observed. With thicker capping (100 nm), the absorption increased further. However, the strain relaxation via

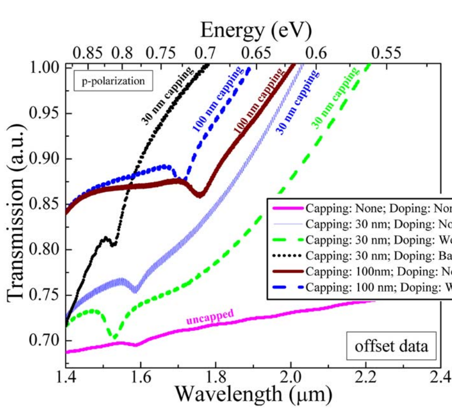

FIG. 4. (Color online) Relative (p-polarization) transmission of undoped, well- or barrier-doped, and uncapped, 30 or 100 nm capped 50 period {1.9-nm-thick GaN/3.2-nm-thick AlN} SL.

cracking is believed to lower the ISB transition energy causing a redshift (Fig. 4). Irrespective of n-doping in barrier or well, ISB transition energy increased (blueshifted) with the addition of doping, due to many-body effects.[20] In conclusion, ISB absorption as low as 1.53 μm—the lowest wavelength reported by MOCVD—is realized and this technique is shown to be appropriate for near-infrared ISB absorption.

In summary, a pulsed MOCVD deposition technique for high optical and structural quality AlN/GaN SL is introduced. Indium is shown to improve the surface and structural quality. Tunability of AlN and GaN thicknesses is demonstrated. ISB absorption at 1.53 μm is achieved at room temperature via MOCVD grown material. Lower (redshift) and higher ISB transition energy (blueshift) is observed in strain-relaxed and well- or barrier-doped SLs, respectively.

The authors would like to thank Dr. D. Silversmith of the AFOSR, Dr. H. Temkin and Dr. M. Rosker of DARPA, Dr. J. Zavada of ARO, and Dr. D. Cardimona of AFRL for discussions and encouragement.

[1]S. Noda, T. Uemure, T. Yamashita, and A. Sasaki, J. Appl. Phys. **68**, 6529 (1990).
[2]I. Vurgaftman and J. R. Meyer, J. Appl. Phys. **89**, 5815 (2001).
[3]J. D. Heber, C. Gmachl, H. M. Ng, and A. Y. Cho, Appl. Phys. Lett. **81**, 1237 (2002).
[4]N. Suzuki and N. Iizuka, Jpn. J. Appl. Phys., Part 2 **36**, L1006 (1997).
[5]C. Gmachl, H. M. Ng, S.-N. G. Chu, and A. Y. Cho, Appl. Phys. Lett. **77**, 3722 (2000).
[6]I. Waki, C. Kumtornkittikul, Y. Shimogaki, and Y. Nakano, Appl. Phys. Lett. **82**, 4465 (2003); **84**, 3703 (2004).
[7]E. Baumann, F. R. Giorgetta, D. Hofstetter, S. Golka, W. Scherenk, G. Strasser, L. Kirste, S. Nicolay, E. Feltin, J. F. Carlin, and N. Grandjean, Appl. Phys. Lett. **89**, 041106 (2006).
[8]S. Nicolay, E. Feltin, J.-F. Carlin, N. Grandjean, L. Nevou, F. H. Julien, M. Schmidbauer, T. Remmele, and M. Albrecht, Appl. Phys. Lett. **91**, 061927 (2007).
[9]A. D. Bykhovski, B. L. Gelmont, and M. S. Shur, J. Appl. Phys. **81**, 6332 (1997).
[10]N. Suzuki, N. Iizuka, and K. Kaneko, Jpn. J. Appl. Phys., Part 1 **42**, 132 (2003).
[11]C. Adelmann, E. Sarigiannidou, D. Jalabert, Y. Hori, J.-L. Rouviere, B. Daudin, S. Fanget, C. Bru-Chevallier, T. Shibata, and M. Tanaka, Appl. Phys. Lett. **82**, 4154 (2003).
[12]P. Boguslawski, K. Rapcewicz, and J. J. Bernholc, Phys. Rev. B **61**, 10820 (2000).
[13]N. Gogneau, D. Jalabert, E. Monroy, E. Sarigiannidou, J. L. Rouviere, T. Shibata, M. Tanaka, J. M. Gerard, and B. Daudin, J. Appl. Phys. **96**, 1104 (2004).
[14]K. Kishino, A. Kikuchi, H. Kanazawa, and T. Tachibana, Appl. Phys. Lett. **81**, 1234 (2002).
[15]C. Bayram, J. L. Pau, R. McClintock, and M. Razeghi, J. Appl. Phys. **104**, 083512 (2008).
[16]C. H. Chen, H. Liu, D. Steigerwald, W. Imler, C. P. Kuo, and M. G. Craford, J. Electron. Mater. **25**, 1004 (1996).
[17]H. J. Kim, S. Choi, D. Yoo, J.-H. Ryou, R. S. Dupuis, R. F. Dalmau, P. Lu, and Z. Sitar, Appl. Phys. Lett. **93**, 022103 (2008).
[18]S. Nicolay, E. Feltin, J.-F. Carlin, M. Mosca, L. Nevou, M. Tchernycheva, F. H. Julien, M. Ilegems, and N. Grandjean, Appl. Phys. Lett. **88**, 151902 (2006).
[19]S. Zhou, M. F. Wu, S. D. Yao, B. S. Zhang, and H. Yang, Superlattices Microstruct. **40**, 137 (2006).
[20]P. K. Kandaswamy, F. Guillot, E. Bellet-Amalric, E. Monroy, L. Nevou, M. Tchernycheva, A. Michon, F. H. Julien, E. Baumann, F. R. Giorgetta, D. Hofstetter, T. Remmele, M. Albrecht, S. Birner, and L. S. Dang, J. Appl. Phys. **104**, 093501 (2008).